Orbital polarization of the conduction electrons in ferromagnetically ordered $GdAl_2$

Michael Bauer
Physikalisches Institut, Universität Bayreuth, Postfach 101251, D-8580 Bayreuth, Germany

M. S. S. Brooks
Commission of the European Communities, Joint Research Centre, Institute for Transuranium Elements, Postfach 2340, D-7500 Karlsruhe, Germany

Elmar Dormann
Physikalisches Institut, Universität Karlsruhe, Postfach 6980, D-7500 Karlsruhe 1, Germany
(Received 25 September 1992)

The anisotropy of the magnetic hyperfine interaction for ^{27}Al nuclei in ferromagnetically ordered $GdAl_2$ is determined for $T \leq 0.7T_c$ using NMR on a single crystalline sphere. The pseudodipolar contribution amounts to about 12% of the dipolar contribution and depends linearly on the temperature-dependent magnetization. The temperature dependence of the quadrupolar splitting for the ^{27}Al a site and for magnetization oriented along the [111] direction is measured from $T=4.2$ K up to the paramagnetic range. It also varies linearly with the magnetization. With the help of relativistic energy-band-structure calculations, we examine the important role of the orbital polarization of the conduction electrons in the ferromagnetically ordered state for these phenomena. These numerical results also give an explanation of the anomalies reported earlier for the ^{27}Al Knight shift and the ^{157}Gd quadrupolar splitting in the ferromagnetic state of cubic Laves-phase structured $GdAl_2$.

I. INTRODUCTION

Reports of NMR in ferromagnetically ordered $GdAl_2$ date back to 1965, when Budnick, Gegenwarth, and Wernick[1] presented the results of their measurements on the ^{27}Al, ^{155}Gd, and ^{157}Gd nuclei in zero external field on powder samples. Since then, a large number of investigations contributed to our growing knowledge about the electronic structure of this "simple" cubic, Laves-phase structured compound.[2] Nevertheless, there are a number of puzzles left, where the experimental results could not be explained within a satisfactory theoretical framework.

The high-field NMR Knight shift was measured for ^{27}Al and ^{157}Gd in a ferromagnetically ordered single crystalline sphere of $GdAl_2$.[3] A change in sign of the ^{27}Al Knight shift in the ferromagnetically ordered state[3] compared to the earlier results for the paramagnetic state was found[4–6] to indicate important rearrangement of the electronic band structure upon magnetic ordering. The necessary band-structure calculations were, however lacking.

In spite of the fact that the Gd ions reside on sites of cubic symmetry in $GdAl_2$ and are generally assumed to have a half-filled (and thus spherical) $4f$ shell, an electric-field gradient (EFG) was observed at the Gd nuclei[7] in the ferromagnetically ordered state of $GdAl_2$. Only about half of the quadrupolar splitting could be explained by the isotropic relativistic single-ion contribution and the influence of magnetostriction, the remaining portion was attached to the magnetically induced EFG due to non-s Gd conduction electrons, but, again, a quantitative theoretical estimate of this contribution is lacking.

The third puzzle concerns the anisotropy of the hyperfine interaction of the ^{27}Al nuclei in the ferromagnetically ordered state of $GdAl_2$, i.e., the observation of an anisotropic transferred hyperfine field[8,9] and of a temperature or magnetization-dependent EFG contribution at the ^{27}Al nucleus.[10–15] This is the main topic of our contribution.

We want to show in this contribution, that the various puzzles mentioned above can be explained by the orbital polarization of the conduction electrons in the ferromagnetically ordered state of $GdAl_2$—or, expressing it in other terms, by the influence of the magnetic order on the electronic densities and currents in $GdAl_2$. Therefore, we extend the experimental basis concerning the anisotropic hyperfine interaction of ^{27}Al in the ferromagnetic state of $GdAl_2$ by the detailed NMR analysis with help of a single crystalline sphere. These results are reported in Sec. IV, after a short description of the relevant theory in II and of the experimental details in Sec. III. In Sec. V we present the theoretical analysis of the orbital contribution, divided into the results of an appropriate energy-band-structure calculation in Sec. V A and the comparison with the experimental results in Sec. V B. The concluding remarks follow in Sec. VI.

II. ANISOTROPIC ^{27}Al HYPERFINE INTERACTION IN $GdAl_2$

The crystallographically equivalent aluminum sites of $GdAl_2$ have axial symmetry ($\bar{3}m$) in the cubic Laves-phase structure. They can be split in up to four magnetically inequivalent sites a, b, c, and d, depending on the orientation of the magnetization with respect to the crys-

tal axes.[8] In the ferromagnetically ordered state, the resonance field can be calculated via

$$\nu_{\rm res}=(\gamma/2\pi)H_{\rm res} \tag{1}$$

from the resonance frequency, using the well-known gyromagnetic ratio $^{27}\gamma/2\pi=1.109\,36$ MHz/kOe:

$$\mathbf{H}_{\rm res}=(1+K)[\mathbf{H}_0-\tilde{N}\mathbf{M}(\mathbf{H}_0)+4\pi\mathbf{M}_S/3]+\mathbf{H}_{\rm hf}+\mathbf{H}_d \tag{2}$$

Here, $\mathbf{H}_0$ is the external field, which is modified internally by the field, temperature, and shape-dependent demagnetizing field ($\tilde{N}$: demagnetization tensor). For a magnetically saturated $GdAl_2$ sphere, demagnetizing and Lorentz field cancel. The Knight shift $K(T\rightarrow 0)=-25\times10^{-4}$ is known and small.[3] For rare-earth intermetallic compounds, it is usual to separate the "classical" point-dipole field $\mathbf{H}_d$ from the hyperfine field $\mathbf{H}_{\rm hf}$. The absolute value and the orientation dependence of $\mathbf{H}_d$ were calculated before.[8,14] It is convenient and usually sufficient to consider only the pseudodipolar part of the anisotropy of the hyperfine field $\mathbf{H}_{\rm hf}$. Thus, for the magnetically saturated sphere,

$$\mathbf{H}_{\rm res}=(1+K)\mathbf{H}_0+\mathbf{H}_{\rm hf,iso}+\alpha\mathbf{H}_d\ , \tag{3}$$

where the pseudodipolar field is taken into account as

$$\mathbf{H}_{\rm pd}=(\alpha-1)\mathbf{H}_d\ . \tag{3a}$$

From NMR measurements on powder samples at 4.2 K, a value of $\alpha\approx1.13$ was estimated for $GdAl_2$.[8] A more clear cut, but corresponding, result was obtained in the first NMR measurements at a magnetically saturated single crystalline $GdAl_2$ sphere at 4.2 K, reported by Fekete *et al.*[9] This pseudodipolar contribution cannot be explained within the framework of a Ruderman-Kittel-Kasuya-Yosida (RKKY) -like polarization of *s*-like conduction electrons. Pseudodipolar contributions on ^{19}F sites caused by polarized *p* orbitals are a familiar result of electron-nuclear double-resonance (ENDOR) studies for rare-earth ions in CaF_2 and related crystals,[16] however. The temperature dependence of α for $GdAl_2$ was not previously known, but will be analyzed in this contribution.

The nuclear quadrupole interaction of ^{27}Al ($I=\frac{5}{2}$) in ferromagnetically ordered $GdAl_2$ has already attracted considerable attention. The pioneering measurements at powder samples in the temperature range from 4.2 to 112 K by Degani and Kaplan[10] revealed an obviously linear relation between part of the quadrupolar splitting frequency $\Delta\nu_Q$ and the temperature-dependent magnetization $M(T)$. The question of the origin for this EFG contribution is not yet finally settled. The explanation put forward by Zevin and Kaplan[11] of a magnon-induced pseudoquadrupolar contribution was disputed by Gehring and Walker[12] who estimated such a contribution to be one order of magnitude too small. They suggested a temperature-dependent EFG contribution caused by lattice expansion instead. In the accessible temperature range of the experiment,[10] a $T^{3/2}$-depending lattice contribution and the linear dependence on the magnetization obeying Bloch's $T^{3/2}$ law would accidentally give the same variation. The uncommon positive sign and the order of magnitude required for the lattice contribution was recently excluded by Riedi, Dumelow, and Abell[13] based on an analysis of the pressure dependence of the EFG. The only explanation left was the influence of lattice vibrations.[13] With NMR in zero field for powder samples and single crystals, the same authors showed that the "magnetically induced" EFG contribution could not be isotropic but should always have its main axis along the local ⟨111⟩ direction of the Al site.[14] To settle these controversies, EFG data are required and reported here, which are taken for a single-crystal sphere magnetized in the [111] direction and which cover temperatures from the ferromagnetically ordered state to far in the paramagnetic range of the same sample. Thus, the high-temperature value of the EFG is also obtained with an improved accuracy compared to earlier results on powder samples.[5,15]

III. EXPERIMENTAL DETAILS

For the NMR measurements, a single crystalline, highly polished and annealed sphere[3] with 8-mm diameter was used, fulfilling the NMR criteria outlined by Fekete *et al.*[9] It was oriented with help of x rays and the NMR spectrum with its $(1\bar{1}0)$ plane perpendicular to the axis of rotation in the NMR probehead and to the axis of the NMR coil, but parallel to the direction of the external magnetic field. Thus NMR spectra in the main cubic orientations [001], [111], and [110] could conveniently be recorded.

The NMR measurements were performed on a Bruker CXP90 spectrometer equipped with home-built probe heads. The Fourier transform of the spin echo, excited by pulses of 2 and 3 μs lengths and integrated over 50 kHz, was recorded versus frequency or external field strength, respectively, in order to determine the resonance line centers. Magnetic-field dependences were analyzed using the variable field strength of an electromagnet (up to 14 kOe) or fixed field (47 kOe) in a superconducting magnet. Temperature variation (4–500 K, stability better than 0.1 K) was realized with help of an Oxford Instruments CF 1200 continuous flow cryostat or a home-built bath cryostat (4.2 K, 77.4 K).

In order to derive the temperature dependence of α, different procedures were combined.

(i) At 4.2 K and 77.4 K, the resonance frequencies of all ^{27}Al resonance lines (*a*-*d*) were recorded as function of the external field ($0\le H_0\le14$ kOe) for the three main directions [001], [111], and [110]. Examples were reported already earlier.[17,18]

(ii) At selected temperatures, the complete angular variation of the ^{27}Al resonance frequencies for the resonance lines *a*-*d* was determined at fixed magnetic field from spectra recorded with variable frequency—see Fig. 1 for an example.

(iii) For fixed field strength applied in the three main crystal orientations, the ^{27}Al resonance frequencies were derived as function of the temperature from 4.2 up to 125 K (i.e., $0.7T_c$, with $T_c=171$ K), see Fig. 2. This is the fastest procedure to derive α. Accordingly, procedure (iii) gave the largest and (ii) the smallest error bars for the pseudodipolar contribution.

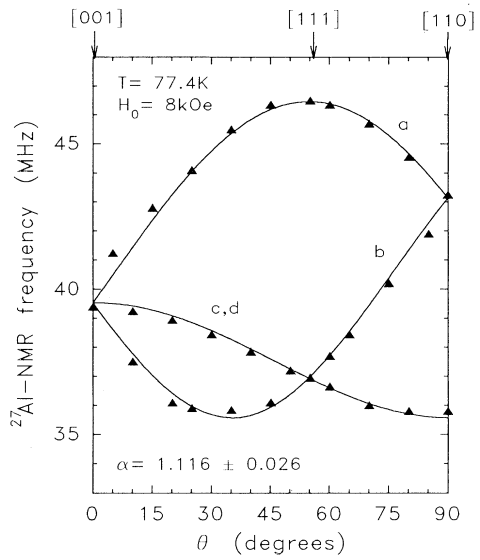

FIG. 1. Angular dependence of the ^{27}Al NMR frequencies in $GdAl_2$ at $T=77.4$ K. The single crystalline sphere was rotated by steps of 5° with the external magnetic field $H_0=8$ kOe in the $(1\bar{1}0)$ plane. The solid line shows the fit with Eq. (3).

The quadrupole splitting frequency for the ^{27}Al NMR line "a" $\Delta\nu_Q([111])$ (i.e., for external field parallel to [111] and the local Al ⟨111⟩ symmetry direction) had to be derived by analysis of the spin-echo amplitude modulation[19] recorded for varied pulse separation at fixed field and frequency (Fig. 3). The direct analysis of the NMR spectrum for the ^{27}Al-a line (recorded as function of field or frequency like shown in Fig. 3 of Ref. 3) did not yield

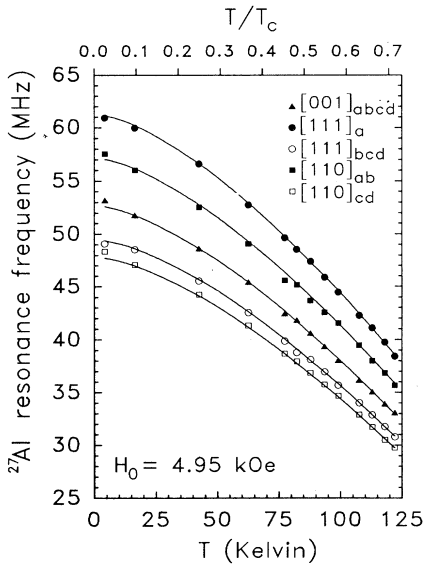

FIG. 2. Temperature dependence of the different ^{27}Al-NMR frequencies (line center) for a magnetic field $H_0=4.95$ kOe applied along the crystallographic axes indicated in the figure. (For $T=4.2$ K only, H_0 is not yet sufficient for magnetic saturation.) The solid lines show the fit with Eqs. (3)–(5), assuming a temperature-independent value of α.

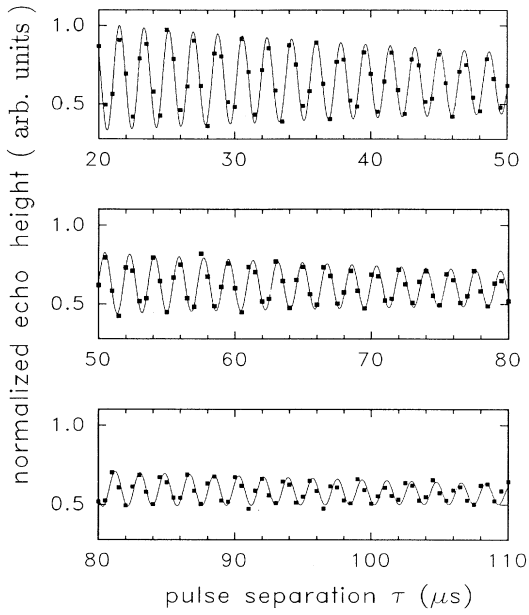

FIG. 3. Spin-echo amplitude (modulation) versus separation of the pulse pair for the ^{27}Al-a site in a ferromagnetically ordered $GdAl_2$ sphere at $T=42.6$ K. The magnetic field $H_0=5.25$ kOe was applied along the [111] direction ($\nu=56.4$ MHz). The solid line fit was obtained for $\Delta\nu_Q=(552.5\pm4.5)$ kHz and a transversal relaxation time $T_2=1.08$ ms.

an accuracy sufficient for the present discussions. The broadening of the resonance lines by an eventual distribution of magnetic resonance fields does not influence the resolution for the spin-echo modulation technique, fortunately. Echo amplitude modulation was recorded for $4.2\text{ K}\leq T\leq 122$ K and temperatures in the paramagnetic range (294.5, 350.1, and 388.9 K). In the high-temperature range, the echo had to be accumulated up to 40 000 times to give a sufficient signal to noise ratio. For the derivation of the quadrupole splitting $\Delta\nu_Q$ (and the transversal relaxation time T_2) from data as shown in Fig. 3, the initial experimentally inaccessible part of the modulated echo amplitude decay was reconstructed as introduced in Ref. 20. The maximal error bar for $\Delta\nu_Q$ thus amounted to ±5.2 kHz in the ferromagnetic and ±7.7 kHz in the paramagnetic phase. For additional information on the experimental details see Ref. 21.

IV. DISCUSSION OF THE EXPERIMENTAL RESULTS

Let us first focus on the anisotropy of the magnetic hyperfine interaction for ^{27}Al in $GdAl_2$. Applying the different experimental procedures (i)–(iii) for the determination of the anisotropy, we found no contradiction to a description with a pseudodipolar contribution, i.e., by adjustment of the parameter α, Eqs. (3) and (3a). Adopting procedure (i), the values $\alpha(4.2\text{ K})=1.13\pm0.05$ and $\alpha(77.4\text{ K})=1.10\pm0.03$ were derived. The time consuming detailed analysis of the angular dependence, procedure (ii) (Fig. 1) gave the value $\alpha(77.4\text{ K})=1.116\pm0.026$. For the analysis of the temperature-

dependence data, the experimentally established scaling[22] for $T \leq 0.7T_c$ was used, i.e.,

$$\frac{H_{\rm hf}(H_i,T)}{H_{\rm hf}(0,0)} = \frac{H_d(H_i,T)}{H_d(0,0)} = \frac{M(H_i,T)}{M(0,0)} \tag{4}$$

with $\mathbf{H}_i = \mathbf{H}_0 - \tilde{N}\mathbf{M}$. In order to calculate the temperature- and field-dependent sample magnetization (considering the influence of thermally excited spin waves and of the exchange polarized conduction electrons) the relations introduced and the relevant parameters determined by Lee and Montenegro[23] were used.

Since the α values at 4.2 and 77.4 K indicated at most a weak temperature dependence of α, all the data derived as function of temperature for different fixed orientations and the fixed external field strength $H_0 = 4.95$ kOe (Fig. 2) in the temperature range 4.2–122 K $\approx 0.7T_c$ were fitted assuming a temperature-independent value of α. Thus $\alpha = 1.12 \pm 0.02$ was obtained [procedure (iii)]. The same value $\alpha = 1.12 \pm 0.02$ is also the average of all individual fixed-temperature data (Fig. 4), proving the consistency of the fitting procedure. The variation of the pseudodipolar contribution as function of the normalized magnetization is plotted in Fig. 5.

Thus the classical point dipole field at the Al sites, calculated for Gd moments of $7.0\mu_B$, is increased by $(12 \pm 2)\%$ in ferromagnetically ordered $GdAl_2$. This effect cannot be spurious and caused by the underestimation of the point dipole contribution by the assumption of too small a Gd moment: experimentally, values of $7.20\mu_B$ (Ref. 23) or $7.06\mu_B$ (Ref. 24) were derived, only slightly larger than the free-ion moment.

In ESR-ENDOR studies of the transferred hyperfine interaction (superhyperfine interaction) at the nonmagnetic (halide) partner in partly covalently bound nonmetallic crystals like the difluorides, containing trivalent rare-earth ions, pseudodipolar contributions were generally observed. They were traced back to the orbital polarization of p electrons at the halide site. It is thus sensible to suggest that an orbital polarization at the Al sites might also be induced in the ferromagnetically ordered state of the intermetallic compound $GdAl_2$. An analysis of the orbital polarization will be made in Sec. V after further evidence for a nonspherical conduction electron distribution obtained from the analysis of the EFG.

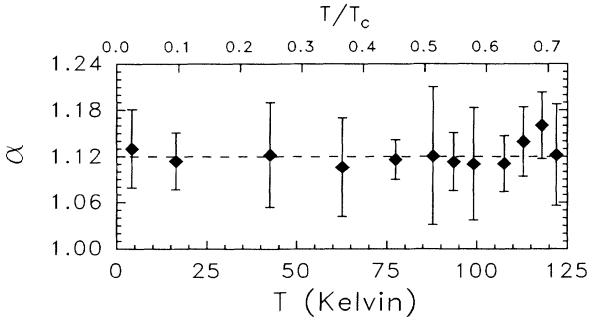

FIG. 4. Temperature dependence of the scaling factor $\alpha = (H_d + H_{\rm pd})/H_d$. Within the error limit, the pseudodipolar contribution has the same temperature dependence as H_d.

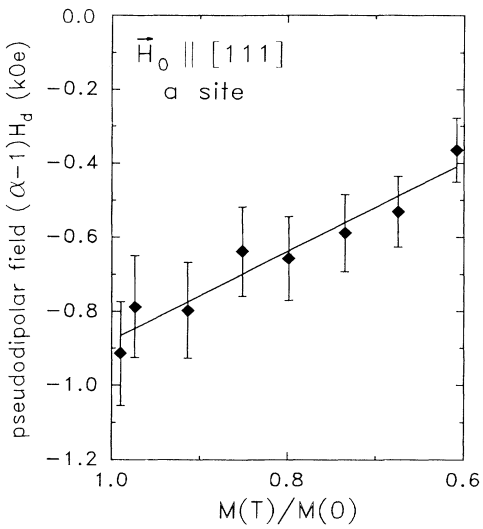

FIG. 5. Pseudodipolar field $H_{\rm pd}$ for the ^{27}Al lattice site a as function of the normalized electronic magnetization $M(T)$ with the temperature as implicit parameter. A linear relation is observed for $T \leq 0.7T_c$.

Figure 6 shows all results for the quadrupole splitting frequency $\Delta\nu_Q$ of the ^{27}Al lattice site a and for magnetization of the single-crystal parallel to the [111] direction, as a function of the normalized magnetization. The temperature, varied between 4.2 and 122 K in the ferromagnetic and 294.5 and 388.9 K in the paramagnetic phase, is the implicit parameter for this representation. The quadrupolar splitting has been fitted by the relation

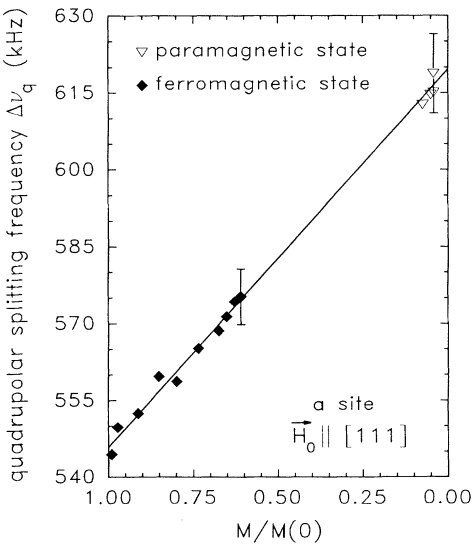

FIG. 6. Quadrupolar splitting frequency $\Delta\nu_Q$ for ^{27}Al on lattice site "a" and magnetic field in [111] direction as function of normalized magnetization in ferromagnetic ($T \leq 0.7T_c$) and paramagnetic phase of $GdAl_2$. A linear dependence (solid line) is clearly established.

$$\Delta\nu_Q([111])=2P=\{619.6-73.8M(H,T)/M(0)\}\ \text{kHz} \tag{5}$$

with an error of ±5.2 kHz. Only the inclusion of the paramagnetic state data allowed for a clear-cut derivation of the actual temperature—or magnetization dependence. The data in the ferromagnetic phase ($T \leq 0.7T_c$) might have been fit to a quadratic dependence on the magnetization or to a $T^{3/2}$ law with only a minor increase in the error limit. The full data set can only be described by the linear dependence on the magnetization. The magnetization-dependent contribution amounts to 12% of the "lattice" contribution, thus, evidently is a non-negligible contribution. By a detailed numerical analysis[21] we ruled out that magnetostriction might explain the magnetization-dependent EFG and pseudodipolar contribution—a magnetostriction of about 10% would be required for the EFG and still be unable to explain $H_{\rm pd}$. But again, an unequal occupation of conduction electron states corresponding at the Al site to different azimuthal character (m_l) of atomic p-like conduction electrons could explain the EFG contribution. Such an orbital contribution was already quoted by Degani and Kaplan.[10] It is actually derived from a relativistic band-structure calculation including spin polarization and spin-orbit coupling as reported in the next section.

V. ORBITAL POLARIZATION IN $GdAl_2$

A. Results of band-structure calculations

The *ab initio* self-consistent energy-band calculations were carried out using the linear-muffin-tin-orbital (LMTO) method[25] in the atomic sphere approximation (ASA) with potentials obtained from the local-spin-density approximation[26] (LSDA) to density-functional theory.[27] For the C15 Laves-phase structure the primitive cell consists of two formula units and, with s, p, and d basis orbitals centered at each of the Gd and Al sites, the LMTO Hamiltonian and overlap matrices are of dimension 54×54 for spin-up or spin-down bands.

A major difficulty with a band-structure treatment of rare-earth metals and their compounds is the combination of the localized $4f$ electron magnetism and the itinerant magnetism of the conduction electrons. Harmon[28] has reviewed the difficulties associated with a density functional treatment of the R-4f states in LSDA. If the number of $4f$ electrons is fixed to an integer, as in the infinite-U limit of the Hubbard model[29] and the total $4f$ spin is also fixed, it is a simple matter to spin polarize the $4f$ density and include the $4f$ spin densities in the total spin density and even though the $4f$ states are not part of the band structure. Details of this procedure are given elsewhere.[30] The total number of $4f$ electrons is known to change from seven for Gd to thirteen for Yb in trivalent compounds. The spin occupation numbers are determined by applying the standard Russel-Saunders coupling scheme to the $4f$ shell. Then S is maximized, L is maximized for a given maximum S, and the total momentum $\mathbf{J}$ is $\mathbf{J}=\mathbf{L}+\mathbf{S}$. The magnetic moment is given by $\boldsymbol{\mu}_f=g_J\mathbf{J}$, where g_J is the Lande factor,

$$g_J=1+\frac{J(J+1)+S(S+1)-L(L+1)}{2J(J+1)}\ . \tag{6}$$

The ground-state spin component of the total $4f$ moment, μ_f^s, is obtained from the projection of the spin along the direction of total angular momentum

$$\mu_f^s=2(g_J-1)J\ . \tag{7}$$

The $4f$ spin-up and spin-down occupation numbers are then determined by

$$n_f=n_f^+ + n_f^-\ ,\quad \mu_f^s=n_f^+ - n_f^-\ , \tag{8}$$

where $n_f^{\pm}$ are the up- and down-spin occupation numbers and n_f is the total number of $4f$ electrons. The foregoing is consistent with the de Gennes factor[31] and model theories of s-f interactions[32] where, at the mean-field level, the projection of the $4f$ spin along the total $4f$ moment direction enters the $4f$-conduction-electron exchange interaction. The constraints are particularly simple for Gd and its compounds where $n_f=n_f^+=7$ and $n_f^-=0$ with $J=S$ and $g_J=2$. Subject to these constraints, the $4f$ spin densities are calculated self-consistently, and the influence of the $4f$ moments upon the magnetism may be obtained. This approach has recently been applied with some success to the $R\mathrm{Fe}_2$ series,[30] the $R\mathrm{Co}_2$ series,[33] and even to the complex magnet $\mathrm{Nd}_2\mathrm{Fe}_{14}\mathrm{B}$ series.[34,35]

Since Al is nonmagnetic the magnetism in $GdAl_2$ is driven by the localized Gd $4f$ spin. The mechanism leading to long-range order may be separated into two distinct parts. Firstly, in the LSDA, the Gd-$4f$ spin density polarizes the Gd $6s$, $6p$, and $5d$ states through local exchange interactions but is otherwise isolated from the conduction-electron environment. The dominant interaction here is between the $4f$ and $5d$ states, since the number, and partial state density at the Fermi energy, of $6s$ and $6p$ electrons is relatively small. The local exchange interaction between R-$4f$ and R-$5d$ states is positive and the corresponding spin moments are always parallel. In fact, this exchange interaction is quite easy to calculate, since the spin-polarization energy in LSDA may be approximated by the expression[36–38]

$$E_{\rm SP}^{\rm LSDA}=-\tfrac{1}{4}\sum_{ll'}J_{l,l'}\mu_l\mu_{l'}\ , \tag{9}$$

where $J_{ll'}$ is an exchange integral[36–38] and μ_l is the lth partial spin moment. The $4f$-$5d$ interaction energy is therefore

$$E_{\rm SP}^{\rm LSDA}(4f-5d)=-\tfrac{1}{2}J_{4f-5d}\mu_{4f}\mu_{5d}\ .$$

The splitting between $5d$ spin-up and spin-down states is then given by

$$\Delta=2\frac{\partial E_{\rm SP}^{\rm LSDA}(4f-5d)}{\partial m_{5d}}=J_{4f-5d}\mu_{4f}\ ,$$

and the induced $5d$ moment is Δ times $N_{5d}(E_F)$, where $N_{5d}(E_F)$ is the partial-$5d$-state density at the Fermi energy per atom and per spin. The exchange integral J_{4f-5d} is 103 meV in a free Gd atom,[36] 92 meV in Gd metal[39]

and 102 meV in $GdAl_2$. Since the Gd spin moment is 7, the splitting of the 5*d* conduction-electron states is about 700 meV or 51 mRy. The calculated partial 5*d*-state density at the Fermi energy for paramagnetic $GdAl_2$ (i.e., with $m_{4f}=0$) is about 12 states per Ry, Gd atom and spin. The estimated 5*d* moment is then about $0.5\mu_B$ per Gd atom.

What actually happens as $GdAl_2$ polarizes is similar to the situation in Gd metal.[39] The state density at the Fermi energy drops as the spin-up and spin-down bands split apart and the partial-5*d*-state density reaches a lower value of about 4 states per Ry, Gd atom and spin when polarization is complete. Hence, the value of the 5*d* moment obtained from the self-consistent calculations is $0.41\mu_B$ and somewhat less than the value estimated from Stoner-type theory above.

Measurements[23,40] suggest that the total moment in $GdAl_2$ is $7.25\mu_B$/f.u., whereas we calculate a moment of almost $7.5\mu_B$/f.u. in the spin polarized calculations. The measured value is anomalous, as has been remarked upon by several authors.[23,40] It has even been suggested that $GdAl_2$ is not a ferromagnet. However, since there appears to be no reason why the localized Gd moment should be less than $7\mu_B$ per Gd we are compelled to use this value as an input to the calculations, in which case no energy-band calculation could possibly yield a conduction-electron moment of as little as is $0.25\mu_B$/f.u. Similar calculations[30,33] for other rare-earth intermetallics yield the conduction-electron moments accurately, and we suspect that the suggestion by Abell *et al.*[40] that $GdAl_2$ is not a true ferromagnet may be correct. (Also, vacancies on Gd sites might reduce the average moment per Gd site derived experimentally.)

In rare-earth transition-metal intermetallics the rare earth (with its chemically inert 4*f* electrons) is an early transition metal in the sense that its 5*d* bands are just beginning to fill. When the transition metal is a late transition metal, the *spins* on the transition-metal and rare-earth sites are coupled antiparallel. The total moments on the atoms will be parallel if the orbital moment of the rare earth is opposite to, and greater than, the spin. The mechanism for this ferromagnetic coupling is *R*-5*d* *M*-3*d* hybridization. Since the gap between the unhybridized spin-down *R*-5*d* and *M*-3*d* bands is smaller than between the unhybridized spin-up bands, hybridization and spin transfer are greater for the spin-down bands, and the interaction between the *M*-3*d* and *R*-5*d* moments is ferrimagnetic.[30,41] However, $GdAl_2$ is a different case, since Al is a broad *sp*-band metal. In the compound, the Gd 5*d* derived bands actually cut the bottom of the broad Al *sp* derived bands and both components of the compound are metals with their bands just beginning to fill. The *spins* on the Al and rare-earth sites are therefore coupled *parallel* in this compound.

Spin-orbit interaction is important whenever orbital magnetism is under investigation. In a second series of calculations the energy bands were not only spin polarized, but the spin-orbit interaction was added to the LMTO Hamiltonian matrix. In contrast to normal-spin-polarized energy-band calculations, where the spin-up and spin-down bands are calculated separately, the spin-up and spin-down bands are connected by matrix elements of the spin-orbit interaction and the size of the relativistic LMTO Hamiltonian becomes 108×108 for $GdAl_2$. Fortunately the relativistic calculations need be iterated no more than twice, but at this stage computer time becomes a serious limitation upon the accuracy of Brillouin zone sampling. The results shown in Table I were for a sample of 178 *k* points and, although the overall description of the electronic structure is no doubt correct, it was not possible to test if details were converged in *k* space.

TABLE I. Partial magnetic moments, atomic orbital occupation numbers, and partial densities of states at Fermi energy according to band-structure calculation.

		^{27}Al	^{157}Gd
μ_s/μ_B		+0.0142	+0.4399
μ_l/μ_B		−0.0050	−0.0425
n_{lm}, $l=1$; $m_l=$	−1	0.5295	0.3739
3*p*(Al)	0	0.5498	0.3593
6*p*(Gd)	+1	0.5247	0.3467
n_{lm}, $l=2$; $m_l=$	−2	0.0587	0.3177
3*d*(Al)	−1	0.0558	0.2648
5*d*(Gd)	0	0.0511	0.3161
	+1	0.0554	0.2661
	+2	0.0590	0.3095
DOS(↑)/Ry^{-1}	*s*	0.175	0.668
	p	2.096	0.722
	d	1.887	10.753
DOS(↓)/Ry^{-1}	*s*	0.454	0.325
	p	6.667	1.517
	d	2.353	8.772

The introduction of spin-orbit interaction does not appreciably change the charge or spin densities. Its main effect is to induce small orbital contributions to the conduction-band moments. The spin-orbit parameter for the Gd 6*p* and 5*d* states were calculated to be 1.25 eV and 0.1 eV, respectively. The spin-orbit parameter for the Al 3*p* was calculated to be 0.016 eV. Although the spin-orbit interaction for the Al 3*p* states is very small, an orbital moment may be induced at the Al site through hybridization with spin-orbit split states at the Gd site. Since the spin moments at the Gd and Al sites are aligned parallel and all sets of basis orbitals are less than half filled, the induced orbital moments at both sites are *antiparallel* to the spin moments.

The detailed numerical results, compiled in Table I, are related to the measurements in the following subsection.

B. Comparison with experimental results

The energy-band-structure calculations indicate a small orbital moment at the Al sites of ferromagnetically ordered $GdAl_2$ (Table I). It is possible that the calculation overestimates the total conduction-electron-spin moment by a factor 2 as mentioned previously, but even if the total moment measurements are not misleading the calculations yield the correct sign and order of magnitude.

The contribution of the Al-p electrons with an azimuthal quantum number m_l (partial occupation number n_{lm}, $l=1$, $m=+1,0,-1$) to the quadrupole splitting frequency can be calculated as[16]

$$\Delta\nu_Q = 2P = \frac{3e^2qQ}{2I(2I-1)h} = \frac{e^2Q\langle r^{-3}\rangle}{I(2I-1)h}\sum_{m_l} n_{lm}(3m_l^2-2) , \tag{10}$$

using $\langle r^{-3}\rangle_{3p}=8.64\times10^{24}$ cm^{-3} (Ref. 42) and the known quadrupole moment Q (Ref. 2). The band-structure-calculations indicate also a nonnegligible Al-3d contribution, which was considered as well [$\langle r^{-3}\rangle_{3d}=2.63\times10^{25}$ cm^{-3} (Ref. 42)]. Thus we determine for ^{27}Al a magnetically induced contribution $\Delta\nu_Q=26.9$ kHz, which shows the correct order of magnitude in comparison with the observed value of 73.8 kHz.

For the nominally cubic Gadolinium site, the quadrupole splitting for ^{155}Gd and ^{157}Gd was reported before.[7] In the detailed analysis for ^{157}Gd, contributions of 375 kHz and 20 kHz to the quadrupole splitting frequency for [111] direction of the magnetization were traced back to the relativistic single-ion contribution and magnetostriction, respectively, for $T\rightarrow0$ K. About 350 kHz were left for an additional magnetically induced (MI) contribution, depending quadratically on the magnetization. If we consider a linear dependence on sample magnetization for this MI contribution instead, as was observed here for the Al site, calculated and observed temperature dependences are evidently in better agreement than before (Fig. 7). (At the same time, the fitted value of the MI contribution is reduced to about 291 kHz). With the data given in Table I, we calculate a splitting frequency of 165 kHz, in agreement to within a factor of 2 with the experimental result. (Gd nuclear data from Ref. 2, $\langle r^{-3}\rangle_{5d}=1.83\times10^{25}$ cm^{-3},[43] $\langle r^{-3}\rangle_{6p}\approx3.6\times10^{25}$ cm^{-3} estimated from optical data.[42])

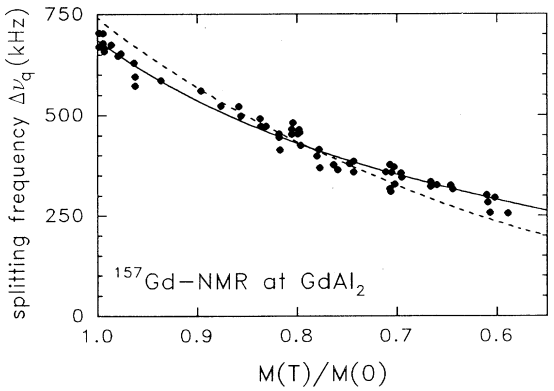

FIG. 7. Quadrupolar splitting frequency $\Delta\nu_Q$ for ^{157}Gd in ferromagnetically ordered $GdAl_2$ as function of normalized magnetization. The data and the broken line fit are taken from Ref. 7. This fit takes the relativistic single ion effect, magnetostriction, and a magnetically induced contribution depending quadratically on $M(T)$ into account. Instead, a linear dependence of the latter effect (corresponding to its origination from orbital polarization of the Gd-conduction electrons) was assumed for the solid line fit.

For the a site and magnetization in [111] direction, the pseudodipolar field of $H_{pd}(T=0)=-0.88$ kOe was derived above. The p-electron orbital contribution can be calculated from the data given in Table I as[44]

$$H_{orb} = -2\mu_B\langle r^{-3}\rangle_{3p}\langle m_l\rangle . \tag{11}$$

The calculated value of -0.80 kOe is in surprisingly close, and probably fortuitous, agreement.

Finally, the Knight shift K for ^{27}Al and ^{157}Gd can be considered for the ferromagnetically ordered state. The necessary hyperfine-coupling constants are compiled in Ref. 3, together with the experimental K values. As can be seen from the drastic differences of spin-up and spin-down densities of states, the influence of the ferromagnetic order on the density of states at the Fermi level is rather pronounced. The susceptibilities χ_i ($i=s,p,d$) entering in the Knight-shift expressions were estimated as[45]

$$\chi_i = g^2\mu_B^2[\mathrm{DOS}(\uparrow)_i^{-1}+\mathrm{DOS}(\downarrow)_i^{-1}]^{-1} , \tag{12}$$

where DOS is the density of states (neglecting the molecular field exchange constant). For ^{157}Gd, a spin contribution to K of -25×10^{-4} is calculated, while a total Knight shift of $K=+52\times10^{-4}$ was observed. This leaves about $+75\times10^{-4}$ for the positive orbital or van Vleck contribution to K, which does not seem unreasonable.[2] For ^{27}Al, a calculated value of $K=-3\times10^{-4}$ has to be compared with the experimental value $K=-25\times10^{-4}$, supporting the observed sign change relative to the paramagnetic state of $GdAl_2$ ($K=+5.5\times10^{-4}$).

Evidently, more detailed band-structure calculations considering different orientations of the Gd moment with respect to the symmetry axis of the crystal are required for a more reliable comparison between experiment and theory. The present stage of the analysis already reveals however, that the experimentally observed puzzles for ferromagnetically ordered $GdAl_2$ are indeed related to the spin and orbital conduction-electron polarization in ferromagnetically ordered $GdAl_2$. Relevant changes in the spin density and current distribution upon magnetic ordering must be considered in the future.

VI. CONCLUDING REMARKS

By NMR investigation of a single crystalline sphere of $GdAl_2$, a pseudodipolar contribution to the hyperfine field at the ^{27}Al nuclei in the ferromagnetically ordered state was established experimentally. It increases the classical point dipole field, which has been calculated as resulting from the $7\mu_B$-Gd moment of $GdAl_2$ before[8,14] by a temperature-independent portion of $(12\pm2)\%$. This is much larger than the deviation of the measured saturation moment from the nominal value of $7.0\mu_B$ per Gd. Under well-defined experimental conditions, we derived, furthermore, the quadrupolar splitting of the ^{27}Al NMR line of the Laves-phase Al site a, i.e., for magnetization parallel to the local symmetry axis $\langle 111\rangle$ of $GdAl_2$. We proved the linear dependence of the magnetically induced

EFG contribution on the electronic magnetization from 4 K until the paramagnetic range. This contribution amounts to up to 12% of the "lattice" EFG. We have shown that elaborate band-structure calculations are required to compete with the achieved degree of sophistication in the present stage of NMR analysis. Exchange, correlation, and spin-orbit interaction have to be taken into account. In part, our numerical results are still qualitative. But we have shown that the Knight-shift change upon magnetic ordering, the electric-field gradient at the nominally cubic Gd lattice site, and the magnetization-dependent pseudodipolar and quadrupolar contributions at the Al site can be explained, at least in principle. In conclusion, orbital contributions and nonspherical charge distributions seem important even in such simple, cubic intermetallic compounds of rare earths with nontransition-metal partners like ferromagnetically ordered $GdAl_2$.

ACKNOWLEDGMENTS

We thank J. Kübler for stimulating discussions and N. Kaplan supplying the $GdAl_2$ sphere. This work was supported by the Deutsche Forschungsgemeinschaft.

[1]J. I. Budnick, R. E. Gegenwarth, and J. H. Wernick, Bull. Am. Phys. Soc. **10**, 317 (1965).
[2]For references, see E. Dormann, in *Handbook on the Physics and Chemistry of Rare Earths,* edited by K. A. Gschneidner, Jr. and LeRoy Eyring (North-Holland, Amsterdam, 1991), Vol. 14, p. 63–161.
[3]H. Kropp, E. Dormann, A. Grayevsky, and N. Kaplan, J. Phys. F **13**, 207 (1983).
[4]V. Jaccarino, B. Matthias, M. Peter, H. Suhl, and J. H. Wernick, Phys. Rev. Lett. **5**, 251 (1960).
[5]E. D. Jones, and J. I. Budnick, J. Appl. Phys. **37**, 1250 (1966).
[6]R. G. Barnes and E. D. Jones, Solid State Commun. **5**, 285 (1967).
[7]E. Dormann, U. Dressel, H. Kropp, and K. H. J. Buschow, J. Magn. Magn. Mater. **45**, 207 (1984).
[8]N. Kaplan, E. Dormann, K. H. J. Buschow, and D. Lebenbaum, Phys. Rev. B **7**, 40 (1973).
[9]D. Fekete, A. Grayevsky, N. Kaplan, and E. Walker, Solid State Commun. **17**, 573 (1975).
[10]J. Degani and N. Kaplan, Phys. Rev. B **7**, 2132 (1973).
[11]V. Zevin and N. Kaplan, Phys. Rev. B **12**, 4605 (1975).
[12]G. A. Gehring and A. B. Walker, J. Phys. C **14**, 5523 (1981).
[13]P. C. Riedi, T. Dumelow, and J. S. Abell, J. Phys. (Paris) Colloq. **49**, C8-451 (1988).
[14]T. Dumelow, P. C. Riedi, J. S. Abell, and O. Prakash, J. Phys. F **18**, 307 (1988).
[15]Y. B. Barash, J. Barak, and N. Kaplan, Phys. Rev. B **25**, 6616 (1982).
[16]A. Abragam and B. Bleaney, *Electron Paramagnetic Resonance of Transition Ions* (Clarendon, Oxford, 1970).
[17]M. Bauer and E. Dormann, Phys. Lett. A **146**, 55 (1990).
[18]M. Bauer and E. Dormann, J. Magn. Magn. Mater. **104-107**, 1291 (1992).
[19]H. Abe, H. Yasuoka, and A. Hirai, J. Phys. Soc. Jpn. **21**, 77 (1966).
[20]Z. Starčuk, Z. Starčuk, Jr., and H. Halámek, J. Magn. Reson. **86**, 30 (1990).
[21]M. Bauer, Ph.D. thesis, Universität Bayreuth, 1992 (unpublished).
[22]U. Herbst, J. Schraub, E. Dormann, and K. H. J. Buschow, Phys. Status Solidi **61**, 465 (1974).
[23]E. W. Lee and J. F. D. Montenegro, J. Magn. Magn. Mater. **22**, 282 (1981).
[24]E. du Tremolet de Lacheisserie, J. Magn. Magn. Mater. **73**, 289 (1988).
[25]O. K. Andersen, Phys. Rev. B **12**, 3060 (1975); H. L. Skriver, *Muffin Tin Orbitals and Electronic Structure* (Springer-Verlag, Heidelberg, 1983).
[26]U. von Barth and L. Hedin, J. Phys. C **5**, 1629 (1972).
[27]P. Hohenberg and W. Kohn, Phys. Rev. **136**, 864 (1964); W. Kohn and L. J. Sham, Phys. Rev. **140**, A1133 (1965).
[28]B. N. Harmon, J. Phys. (Paris) Colloq. **40**, C5-65 (1979).
[29]J. Hubbard, Proc. R. Soc. London, Ser. A **276**, 238 (1963).
[30]M. S. S. Brooks, L. Nordström, and B. Johansson, J. Phys. Condens. Matter **3**, 2357 (1991).
[31]P. G. de Gennes, J. Phys. Rad. **23**, 510 (1962).
[32]See, e.g., S. H. Liu, in *Handbook on the Physics and Chemistry of Rare Earths,* edited by K. A. Gschneidner, Jr. and L. Eyring (North-Holland, Amsterdam, 1978), Vol. 1, p. 233.
[33]L. Nordström, M. S. S. Brooks, and B. Johansson, J. Appl. Phys. **70**, 6583 (1991).
[34]L. Nordström, M. S. S. Brooks, and B. Johansson, J. Appl. Phys. **69**, 5708 (1991).
[35]K. Hummler and M. Fähnle, Phys. Rev. B **45**, 3161 (1992).
[36]M. S. S. Brooks and B. Johansson, J. Phys. F **13**, L197 (1983).
[37]O. Gunnarsson, J. Phys. F **6**, 587 (1976).
[38]J. F. Janak, Phys. Rev. B **16**, 255 (1977).
[39]M. S. S. Brooks, S. Auluck, T. Gasche, L. Trygg, L. Nordström, L. Severin, and B. Johansson, J. Magn. Magn. Mater. **104-107**, 1496 (1992).
[40]J. S. Abell, J. X. Boucherle, R. Osborn, B. D. Rainford, and J. Schweizer, J. Magn. Magn. Mater. **31-34**, 247 (1983).
[41]I. A. Campbell, J. Phys. F **2**, L47 (1972).
[42]H. Chihara and N. Nakamura, in *NQRS-Data,* edited by K. H. Hellwege and A. M. Hellwege, Landolt-Börnstein, Neue Serie, Zahlenwerte und Funktionen aus Naturwissenschaft und Technik, Vol. III/20a (Springer Verlag, Berlin, 1988); *Atom- und Molekularphysik,* edited by A. Eucken (Springer-Verlag, Berlin, 1950), Vol. I/1.
[43]P. J. Unsworth, J. Phys. B **2**, 122 (1969).
[44]A. Narath, in *Hyperfine Interactions,* edited by A. J. Freeman and R. B. Frankel (Academic, Oxford, 1967), p. 287.
[45]Ch. Kittel, *Einführung in die Festkörperphysik* (Oldenbourg-Verlag, Müchen, 1983).